Iron-meditated fungal starvation by lupine rhizosphere-associated and extremotolerant *Streptomyces* sp. S29 desferrioxamine production

Scott A. Jarmusch[a,c]*, Diego Lagos-Susaeta[b]†, Emtinan Diab[a]†, Oriana Salazar[b], Juan A. Asenjo[b], Rainer Ebel[a], Marcel Jaspars[a]*

[a] Marine Biodiscovery Centre, Department of Chemistry, University of Aberdeen, Old Aberdeen AB24 3UE, Scotland, U.K.

[b] Centre for Biotechnology and Bioengineering, University of Chile, Beauchef 850, Santiago, Chile.

[c] Department of Pharmaceutical Biosciences – Pharmacognosy, Uppsala University, Biomedicinskt Centrum, Uppsala, Sweden 751 23

†Authors contributed equally to this work

*Corresponding authors: scott.jarmusch@farmbio.uu.se; m.jaspars@abdn.ac.uk

ABSTRACT

Siderophores are iron-chelating compounds that aid iron uptake, one of the key strategies for microorganisms to carve out ecological niches in microbially diverse environments. Desferrioxamines are the principal siderophores produced by *Streptomyces* spp. Their biosynthesis has been well studied and as a consequence, the chemical potential of the pathway continues to expand. With all of this in mind, our study aimed to explore extremotolerant and Lupine rhizosphere-derived *Streptomyces* sp. S29 for its potential antifungal capabilities. Cocultivation of isolate S29 was carried out with *Aspergillus niger* and *Botrytis cinerea*, both costly fungal phytopathogens in the wine industry, to simulate their interaction within the rhizosphere. The results indicate that not only is *Streptomyces* sp. S29 extraordinary at producing hydroxamate siderophores but uses siderophore production as a means to 'starve' the fungi of iron. High resolution LC-MS/MS followed by GNPS molecular networking was used to observe the datasets for desferrioxamines and guided structure elucidation of new desferrioxamine analogues. Comparing the new chemistry, using tools like molecular networking and MS2LDA, with the known biosynthesis, we show that the chemical potential of the desferrioxamine pathway has further room for exploration.

INTRODUCTION

The application of *Streptomyces* secondary metabolites goes beyond drug discovery, as they are one of the most important bacteria for crop protection. Their biotechnological application as rhizosphere or endophytic bacteria is proven to confer protection against soilborne pathogens like fungi, nematodes, and other bacteria.[1,2] They serve as an important factor in 'disease suppressive soils', with several mechanisms of action including synthesis of plant growth regulators[3], antibiotic production[2], secretion of volatile compounds[4], and siderophore production.[5] The last of these is not only a way for bacteria to uptake vital metals from the surrounding soil but also to sequester metals in order to gain a competitive edge against other soilborne organisms.

Rhizosphere-associated microbes are one of the many strategies currently being explored as biocontrol agents. Bacterial communities in the rhizosphere contribute to the extremely complex flow of nutrients as well as the export of antibiotics and other secondary metabolites into the soil.[6,7] Model organisms from genera like *Bacillus* and *Pseudomonas* have traditionally been promising sources due to their association to the soil and their production of secondary metabolites like lipopeptides but also plant growth promotors.[8,9] Actinobacteria, which are also predominantly soil-associated microbes, have also been explored as biocontrol agents due to their prolific antimicrobial potential.[10] This combined with the fact that extremotolerant microbes have adapted to the harsh conditions and the potential of these adaptations to be translatable to biotechnologies, extremotolerant microbes look to be promising sources as biocontrol agents.[11] In Chile, the wine industry is the main agricultural export, estimated at ~$2 billion USD in 2017[12],

55 thus driving a large research interest around protection of wine-producing grapes against
56 various phytopathogens.

57 Siderophores are iron-chelating compounds that aid metal uptake in iron deficient
58 environments.[13] These secondary metabolites are produced by all microbes and four
59 types of siderophore-mediated social interactions have been observed: uptake among
60 clonal cells (sharing), cheating or piracy (which can only happen amongst microbes with
61 the same uptake receptor), competition via locking away and metabolite competition
62 (whichever microbe makes the most cost efficient and effective chelator).[14]
63 Desferrioxamines (DFO) are the most widely observed group of siderophores in
64 *Streptomyces* spp., used principally for Fe(III) scavenging[13,15], as well as some other
65 heavy metals.[16–18] Since the vast majority of organisms require Fe(III) in order to maintain
66 proper cell wall function[13], as one scavenges for itself, it simultaneously starves other
67 competing organisms, rendering them potentially unviable.

68 The biosynthetic machinery of desferrioxamines has been well studied[19–21] and as
69 a consequence, the chemical potential continues to expand. The substrate specificity of
70 DesC-like proteins, similar to acyl CoA-dependent transferases, seems to be the key
71 factor in producing diverse desferrioxamine scaffolds.[19,21] It has been shown that DesC
72 can accommodate for acetyl, succinyl, and myristol-CoA, with the latter providing insight
73 into the production of acyl desferrioxamines.[19] Additionally, aryl desferrioxamines, first
74 isolated from *Micrococcus luteus* KLE1011[22] and later from *Streptomyces* sp. MA37[23],
75 showed further substrate flexibility, where the latter communication described a new
76 biosynthetic gene cluster (BGC) which contained a DesC homolog (LgoC). This enzyme
77 promiscuity fits ideally with the Screening Hypothesis first proposed by Firn and Jones;

78 secondary metabolism stems from metabolic pathways that 'maximize diversity and
79 minimize cost'.[24]

80 Due to the modular nature of desferrioxamines and the presence of peptide bonds
81 throughout their structure, mass spectrometry-based studies have been utilized
82 extensively to not only study their biological impact but also for elucidation of new
83 structures. Previous studies have established standard fragmentation patterns of these
84 siderophores, even as far as elucidating new structures solely based on mass
85 spectrometry.[25–31] This standardized fragmentation makes the discovery of siderophores
86 much easier thanks to metabolomics-based tools like molecular networking, like Global
87 Natural Products Social Molecular Networking (GNPS). Molecular networking allows for
88 correlations to be drawn within your dataset and against the GNPS library that relates
89 similar MS/MS spectra to one another, forming clusters or families of similar features.[32]

90 With all of this in mind, our study originally aimed to explore extremotolerant,
91 rhizosphere-derived *Streptomyces* sp. S29, a novel strain, for antifungal secondary
92 metabolites. Cocultivation of S29 with *Aspergillus niger* and *Botrytis cinerea*, both costly
93 fungal phytopathogens in the wine industry, were carried out in a fashion to allow S29 to
94 dominate the culture, thus eliciting a chemical response from the addition of each fungus.
95 Bioassay-guided fractionation lead to no lead compounds as potential antifungal agents
96 yet post-fermentation streaks of inoculum showed no fungal growth. High resolution LC-
97 MS/MS followed by GNPS molecular networking was used to analyse the data sets. The
98 results indicated that not only is *Streptomyces* sp. S29 extraordinary at producing
99 hydroxamate siderophores, totalling 24 new analogues and 8 previously identified ones
100 confirmed through MS/MS structure elucidation, but uses siderophore production as a

101 means to ‘starve’ the fungi of iron. When grown in coculture with the fungi, 22 additional
102 new analogues and 17 additional previously described were identified, clearly showing a
103 chemical response to the fungi in culture environment. Using MS2LDA to further explore
104 desferrioxamine chemical space, we observed that it is potentially 2.5 times larger than
105 previously anticipated. These results point to the potential of *Streptomyces* sp. S29 as a
106 biocontrol agent to prevent fungal infection and the potential for new desferrioxamine
107 chemistry.

RESULTS AND DISCUSSION

***Streptomyces* sp. S29 cocultivation and LC-MS of desferrioxamine-rich fractions.** Preliminary fungal bioassay screening of the lupine rhizosphere *Streptomyces* culture collection showed a novel strain, *Streptomyces* sp. S29, inhibited the growth of *Botrytis cinerea* when grown in coculture on solid medium (Figure 1). In an attempt to induce production of antifungal metabolites, the bacteria and fungi were cocultivated in liquid culture in a fashion to allow for *Streptomyces* sp. to be the dominant microbe. Bioassay guided fractionation of the *sec*-butanol fraction lead to no antifungal leads even though inhibition was observed against *B. cinerea* only (Figure S6). Upon LC-MS and ^{1}H NMR analysis of the extracts, a profusion of DFOs was observed in all *sec*-butanol fractions, leading to the hypothesis that this *Streptomyces* sp. uses a different mechanism than producing antimycotics to combat the fungal cocultivate, as seen previously in human bacterial infections.[33] DFOs historically have never exhibited antimicrobial activity and therefore we confidently presume they are not responsible for the inhibition seen in Figure S6.[34] *Streptomyces* sp. S29 was also grown in monoculture on iron deficient medium to induce production of DFOs in an attempt to compare siderophore production to the coculture experiments. *Aspergillus niger* and *Botrytis cinerea* were chosen as the fungal phytopathogens due to their established pathology of wine producing grapes [35,36] and the importance of wine as Chile's main agricultural export. Additionally, these fungi would be encountered in *Streptomyces* sp. S29's ecological niche, making this an important evaluation of microbes it would encounter in the soil environment.

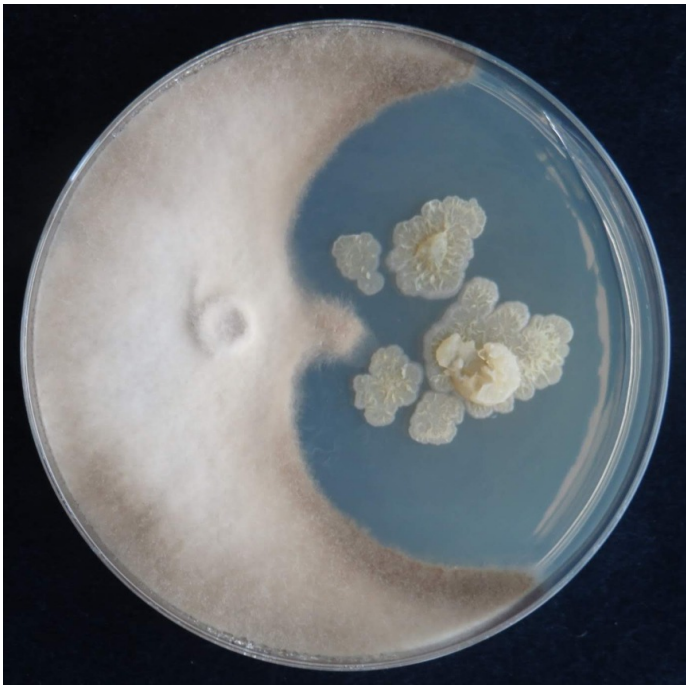

Figure 1. Preliminary antifungal screening on *Streptomyces* isolate S29 (right) grown with *Botrytis cinerea* (left). Image courtesy of Diego Lagos-Susaeta.

Extracts and fractions were evaluated for the presence of two DFOs (B and D1) during the fractionation steps, in order to trace the fractions that contained the highest abundance of siderophores. Presence of DFOs was further evaluated at the final stages of separation based on the molecular families generated from molecular networking, utilizing the known DFOs in the GNPS library as anchor points, which further aided structure elucidation. Based on the LC-MS results, the butanol partitions contained the largest abundance of DFOs, and therefore this data was used to generate a molecular network using GNPS.

Molecular networking and MS/MS based structure elucidation. The molecular network generated contained 1169 molecular features after removal of features originating from media and instrument blanks. Each subnetwork was approached using GNPS library hits as ‘anchors’ (hexagons in each subnetwork) and then collecting the

142 masses of linked nodes and predicting molecular formula from the raw data. Using these
143 'anchors' not only allows one to relate the nodes directly connected to the anchor, but
144 also gives broader sense of the molecular nature of a cluster. The hydroxamate
145 siderophores were primarily distributed amongst three principle molecular families
146 (Figures 2-4). Subnetwork 1 (Figure 2) contained a number of new acyl DFO D-like
147 analogues that are first described in this study as well as new analogues of acyl DFO B-
148 like derivatives. Subnetwork 2 (Figure 3) is mostly composed of unknown derivatives
149 although a suite of new macrocyclised DFOs and tenacibactin derivatives, first described
150 by Jang et al. [37], were observed. The last principle subnetwork contained various Fe(III)
151 and Al(III) complexed FOs (Figure 6). Within this network a new analogue was identified,
152 uC_{12} acyl FO-B, while its non-chelated form was not observed in the data (Figure S32).
153 Aryl desferrioxamines related to the previously described acyl ferrioxamine 1 (also
154 known as legonoxamine A) and 2 were also found distributed amongst varying molecular
155 families across the molecular network and do not seem to link into their own cluster like
156 seen for the DFO-Ds and DFO-Bs. For the remaining small molecular families that contain
157 DFOs, we observed a group of sodiated adducts, large acyl DFO-Bs, as well as the
158 macrocyclised desferrioxamine E (Figure S1). The remaining nodes that link within the
159 desferrioxamine molecular families were unable to be identified using the annotation
160 workflow described in Figure 4.

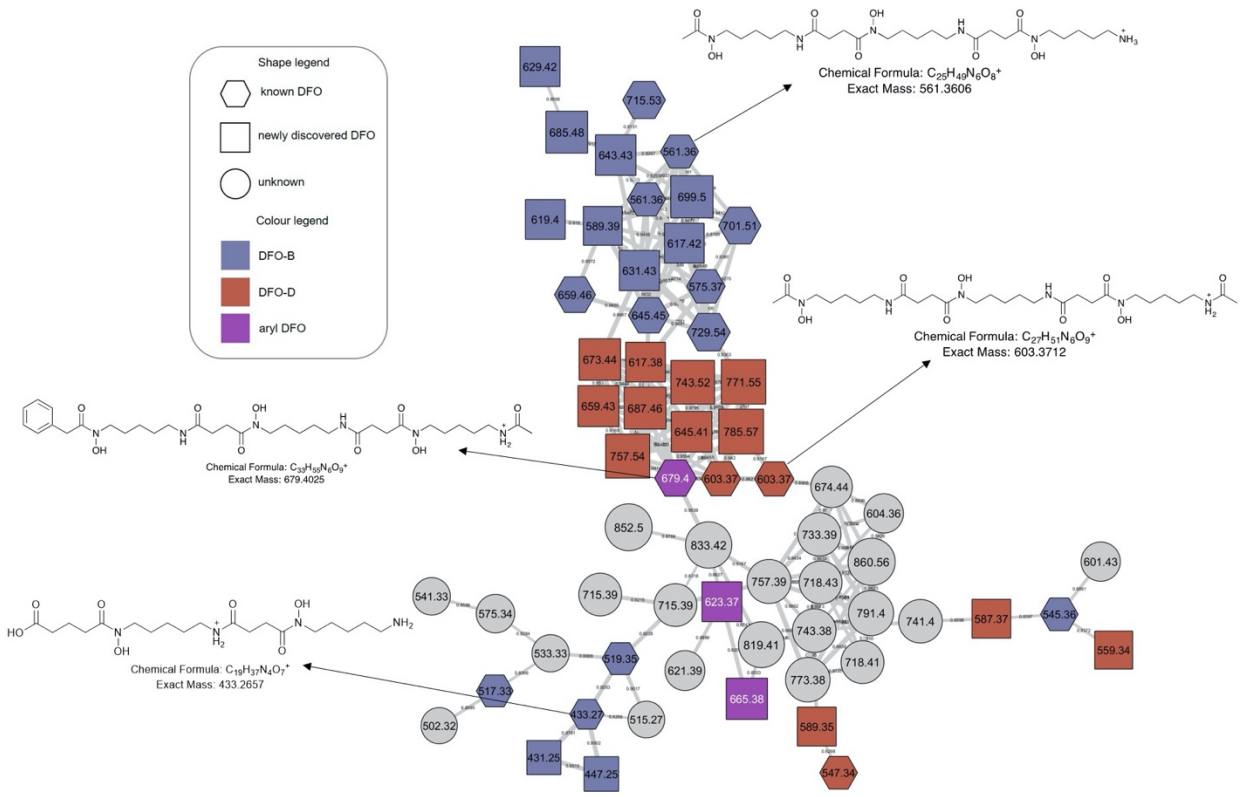

Figure 2. Desferrioxamine subnetwork 1. Distributed amongst the molecular family are DFO-Bs (blue), DFO-Ds (red), and aryl DFOs (purple). Grey nodes represent potential DFOs that were not able to be annotated using MS/MS data only.

161

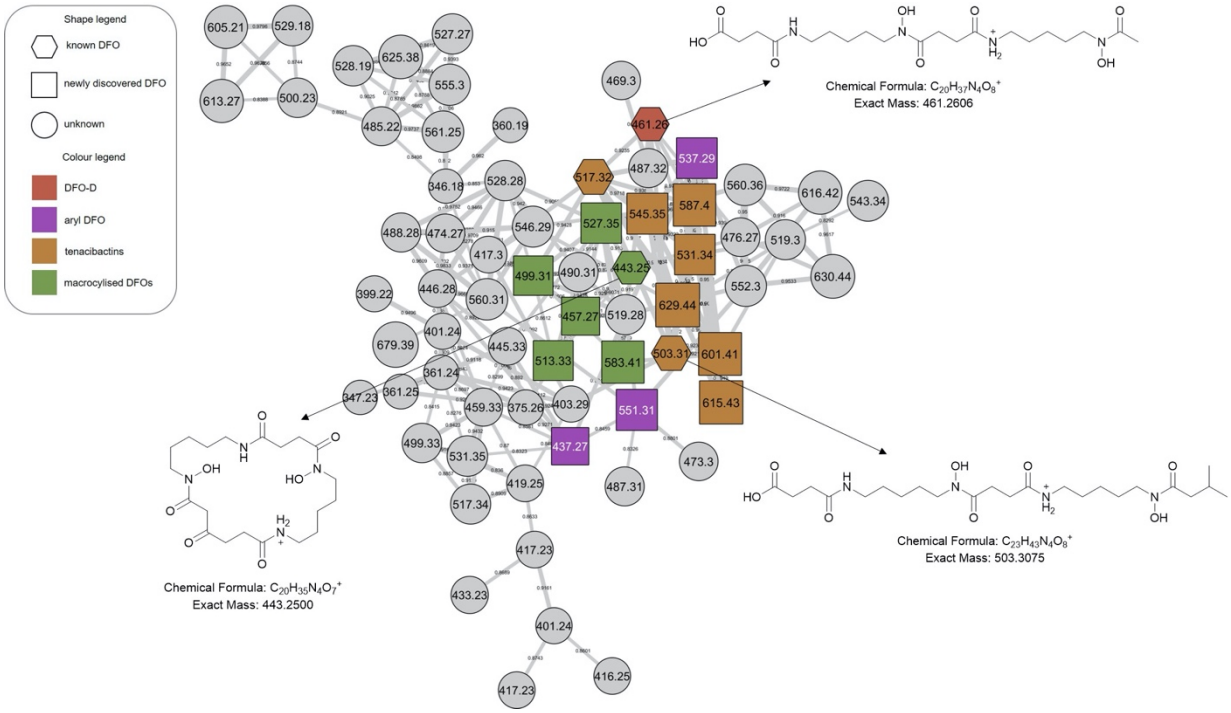

Figure 3. Desferrioxamine subnetwork 2. Within the molecular family are macrocyclised DFOs (green) as well as a number of new tenacibactin derivatives (orange). Grey nodes represent potential DFOs that were not able to be annotated using MS/MS data only.

162

163 MS/MS based structure elucidation was carried out in a similar fashion to studies
164 conducted previously (Figure 4).[25–28] Early observations of desferrioxamine B and D1
165 fragmentation showed an initial loss of the N-terminus, corresponding to the loss of either
166 118.1 or 160.1. Using this as a foundation, structures were either started with a *N*-
167 hydroxycadaverine or a *N*-hydroxy-*N*-acetylcadaverine, respectively. The remainder of
168 structure elucidation was completed stepwise: (1) predicting the molecular formula from
169 the accurate mass and collection of MS/MS data, (2) filling out the structures with
170 appropriate desferrioxamine precursors (i.e. *N*-hydroxycadaverine, putrescine, succinate,
171 acetate, etc.), and (3) taking the remainder of the molecular formula and placing an
172 appropriate acid at the C-terminus that either has precedent from previous studies or
173 could be a potential binding partner with an acyltransferase like coenzyme A.

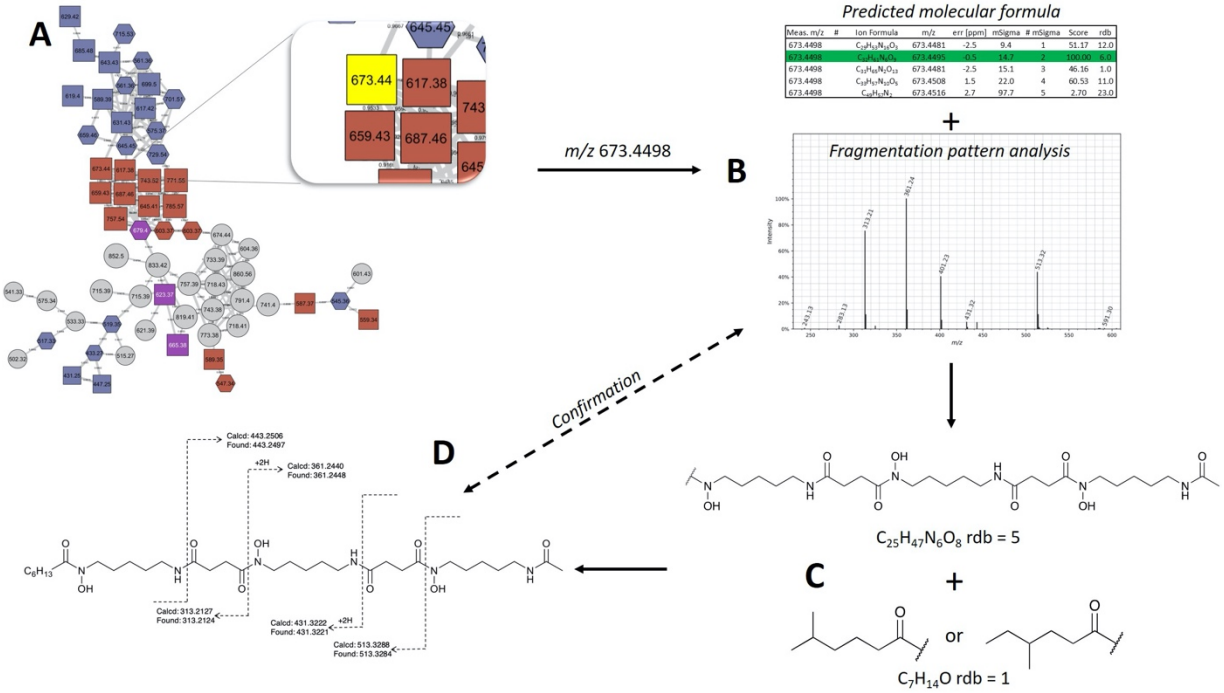

Figure 4. Molecular network and MS/MS based structure determination. (A) molecular networks generated using GNPS were dereplicated and potentially unknown ions were found in the Raw data. (B) Predicted molecular formula were generated and the most likely candidate formula was chosen. MS/MS spectra were analysed for the initial loss of -118 or -160 to determine the N-terminal moiety of *N*-hydroxycadaverine or *N*-acetylhydroxycadaverine, respectively. (C) Based on known structure of desferrioxamines, substructures were proposed for each new metabolite and lastly, (D) putative structures were confirmed using the MS/MS data.

176 Overall, 46 new DFO analogues were identified in the molecular network and
177 through manual data processing (Table 1). These range from short acyl chain DFO-Bs,
178 acyl desferrioxamine D-like (DFO-D) analogues which have not previously been
179 described, tenacibactins, aryl DFOs, macrocylised DFOs, and long chain dicarboxylate
180 DFOs (Table 1). Additionally, 25 known hydroxamate siderophores were detected,
181 including known acyl, aryl DFOs and bisucaberins, giving further credence to the new
182 structure assignments. Their identification and observed presence in monoculture and/or
183 coculture are present in Table 1.

Table 1. Summary of siderophores identified using molecular networking and manual observations of the data. Nomenclature that are italicized were identified in this study.

	Name	Measured mass [M+H]+	Theoretical mass [M+H]+	Δ ppm	Sum formula [+H]+	Monoculture	Reference
cyclic desferrioxamines	Bisu-03	429.2344	429.2342	-0.46	$C_{19}H_{33}N_4O_7$		Senges et al.
	Bisu-01	443.2495	443.2500	-1.13	$C_{20}H_{35}N_4O_7$		Senges et al.
	Bisu-10	457.2660	457.2657	0.65	$C_{21}H_{37}N_4O_7$	*	*This study*
	Bisu-11	499.3110	499.3126	-3.20	$C_{24}H_{43}N_4O_7$	*	*This study*
	Bisu-12	513.3310	513.3283	5.25	$C_{25}H_{45}N_4O_7$	*	*This study*
	Bisu-13	527.3450	527.3439	2.08	$C_{26}H_{47}N_4O_7$	*	*This study*
	Bisu-14	583.4050	583.4065	-2.57	$C_{30}H_{55}N_4O_7$		*This study*
	desferrioxamine E	601.3557	601.3556	0.17	$C_{27}H_{49}N_6O_9$		
aryl desferrioxamines	legonoxamine B	337.1754	337.1758	-1.19	$C_{17}H_{25}N_2O_5$		Maglangit et al.
	legonoxamine C	351.1912	351.1914	-0.57	$C_{18}H_{37}N_4O_5$		*This study*
	legonoxamine D	437.2755	437.2758	-0.69	$C_{22}H_{37}N_4O_5$		*This study*
	legonoxamine E	537.2924	537.2919	0.93	$C_{26}H_{41}N_4O_8$	*	*This study*
	legonoxamine F	551.3088	551.3075	2.36	$C_{27}H_{43}N_4O_8$		*This study*
	legonoxamine G	623.3764	623.3763	0.16	$C_{30}H_{51}N_6O_8$	*	*This study*
	acyl-ferrioxamine 1/ legonoxamine A	637.3917	637.3919	-0.31	$C_{31}H_{53}N_6O_8$	*	D'Onofrio et al; Maglangit et al.
	legonoxamine H	665.3893	665.3869	3.61	$C_{32}H_{53}N_6O_9$		*This study*
	acyl-ferrioxamine 2	679.4025	679.4025	0.00	$C_{33}H_{55}N_6O_9$	*	D'Onofrio et al.
	legonoxamine A glycoside	799.4456	799.4448	1.00	$C_{37}H_{63}N_6O_{13}$	*	*This study*
DFO-Bs	*un-pre[5+5*]*	431.2500	431.2520	-4.63	$C_{19}H_{35}N_4O_7$		*This study*
	pre[5+5*]	433.2662	433.2657	-1.15	$C_{19}H_{37}N_4O_7$		Rütschlin et al.
	pre[5+5] aldehyde*	447.2450	447.2449	0.22	$C_{19}H_{35}N_4O_8$		*This study*
	pre[ha+5+5*]	517.3221	517.3232	-2.12	$C_{24}H_{45}N_4O_8$		Rütschlin et al.
	abloxime / IC202C	517.3347	517.3344	0.58	$C_{23}H_{45}N_6O_7$	*	Iijima et al.
	proferrioxamine G1t	519.3495	519.3501	-1.16	$C_{23}H_{47}N_6O_7$		Feistner et al.
	DesuA1	545.3658	545.3657	0.18	$C_{25}H_{49}N_6O_7$	*	Senges et al.
	DesA1	547.3449	547.3450	-0.18	$C_{24}H_{47}N_6O_8$	*	Senges et al.
	Des A2 / IC202B	557.2880	557.2881	-0.18	$C_{23}H_{43}N_6O_8Al$		Iijima et al.
	desferrioxamine B	561.3602	561.3606	-0.71	$C_{25}H_{49}N_6O_8$	*	
	desferrioxamine N /desf-05	575.3762	575.3763	-0.17	$C_{26}H_{51}N_6O_8$	*	Ejje et al; Senges et al.
	C3 acyl DFO-B	589.3915	589.3919	-0.68	$C_{27}H_{53}N_6O_8$	*	*This study*
	C4 acyl DFO-B	603.4073	603.4076	-0.49	$C_{28}H_{55}N_6O_8$	*	*This study*
	C5 acyl DFO-B	617.4233	617.4232	0.16	$C_{29}H_{57}N_6O_8$	*	*This study*
	C4 acyl hydroxylated DFO-B	619.4024	619.4025	-0.16	$C_{29}H_{55}N_6O_9$	*	*This study*
	uC6 acyl DFO-B	629.4238	629.4232	0.95	$C_{30}H_{57}N_6O_8$		*This study*
	C6 acyl DFO-B	631.4388	631.4389	-0.16	$C_{30}H_{59}N_6O_8$	*	*This study*
	uC7 acyl DFO-B	643.4389	643.4389	0.00	$C_{31}H_{59}N_6O_8$		*This study*
	C7 acyl-DFO	645.4550	645.4545	0.77	$C_{31}H_{61}N_6O_8$		Traxler et al; Sidebottom et al.
	C8 acyl-DFO	659.4697	659.4702	-0.76	$C_{32}H_{63}N_6O_8$		Traxler et al; Sidebottom et al.

Table 1 cont. Summary of siderophores identified using molecular networking and manual observations of the data. Nomenclature that are italicized were identified in this study.

	Name	Measured mass [M+H]+	Theoretical mass [M+H]+	Δ ppm	Sum formula [+H]+	Monoculture	Reference
DFO-Bs	*uC10 acyl DFO-B*	685.4856	685.4858	-0.29	$C_{34}H_{65}N_6O_8$		*This study*
	uC11 acyl DFO-B	699.5007	699.5025	-2.57	$C_{35}H_{69}N_6O_8$		*This study*
	C11 acyl-DFO	701.5174	701.5171	0.43	$C_{35}H_{69}N_6O_8$		Traxler et al; Sidebottom et al.
	C12 acyl-DFO	715.5322	715.5328	-0.84	$C_{36}H_{71}N_6O_8$		Traxler et al; Sidebottom et al.
	C13 acyl-DFO	729.5496	729.5484	1.64	$C_{37}H_{73}N_6O_8$		Traxler et al; Sidebottom et al.
	uC12 acyl FO-B [M+Al]+	737.4776	737.4752	3.25	$C_{36}H_{66}N_6O_8Al$		*This study*
	dodecanedioic DFO-B	745.5086	745.5070	2.15	$C_{36}H_{69}N_6O_{10}$		*This study*
	amphiphilic desferrioxamine 12	745.5438	745.5434	0.54	$C_{37}H_{73}N_6O_9$		Sidebottom et al.
	tridecanedioic DFO-B	759.5221	759.5226	-0.66	$C_{37}H_{71}N_6O_{10}$		*This study*
	amphiphilic desferrioxamine 15	759.5597	759.5590	0.92	$C_{38}H_{75}N_6O_9$		Sidebottom et al.
DFO-Ds	desferrioxamine H	461.2602	461.2606	-0.87	$C_{20}H_{37}N_4O_8$		Adapa et al.
	glutaric desferrioxamine H	475.2760	475.2762	-0.42	$C_{21}H_{39}N_4O_8$		*This study*
	C2 acyl glutaric desferrioxamine H	489.2900	489.2919	-3.88	$C_{22}H_{41}N_4O_8$		*This study*
	desferrioxamine D4	559.3453	559.3450	0.50	$C_{25}H_{47}N_6O_8$		*This study*
	deoxydesferrioxamine D3	587.3757	587.3763	-1.02	$C_{27}H_{51}N_6O_8$	*	*This study*
	Desferrioxamine D3	589.3915	589.3919	-0.68	$C_{27}H_{53}N_6O_8$	*	*This study*
	desferrioxamine D1	603.3714	603.3712	0.33	$C_{27}H_{51}N_6O_9$	*	
	C2 acyl DFO-D	617.3864	617.3869	-0.81	$C_{28}H_{53}N_6O_9$		*This study*
	C4 acyl DFO-D	645.4185	645.4182	0.46	$C_{30}H_{57}N_6O_9$	*	*This study*
	C5 acyl DFO-D	659.4331	659.4338	-1.06	$C_{31}H_{59}N_6O_9$		*This study*
	C6 acyl DFO-D	673.4498	673.4495	0.45	$C_{32}H_{61}N_6O_9$	*	*This study*
	C7 acyl DFO-D	687.4655	687.4651	0.58	$C_{33}H_{63}N_6O_9$	*	*This study*
	C11 acyl DFO-D	743.5280	743.5277	0.40	$C_{37}H_{71}N_6O_9$	*	*This study*
	C12 acyl DFO-D	757.5436	757.5434	0.26	$C_{38}H_{73}N_6O_9$	*	*This study*
	C13 acyl DFO-D	771.5607	771.5590	2.20	$C_{39}H_{75}N_6O_9$	*	*This study*
	C14 acyl DFO-D	785.5749	785.5747	0.25	$C_{40}H_{77}N_6O_9$	*	*This study*
tenacibactins	tenacibactin C	503.3070	503.3075	0.99	$C_{23}H_{43}N_4O_8$		Jang et al.
	tenacibactin E	531.3380	531.3388	-1.15	$C_{25}H_{47}N_4O_8$	*	*This study*
	tenacibactin F	545.3545	545.3545	0.00	$C_{26}H_{49}N_4O_8$	*	*This study*
	tenacibactin G	587.3990	587.4014	4.08	$C_{29}H_{55}N_4O_8$		*This study*
	tenacibactin H	601.4168	601.4171	-0.49	$C_{30}H_{57}N_4O_8$	*	*This study*
	tenacibactin I	615.4326	615.4327	-0.16	$C_{31}H_{59}N_4O_8$		*This study*
	tenacibactin J	629.4484	629.4484	0.00	$C_{32}H_{61}N_4O_8$		*This study*

184

185 **Acyl DFO production by *Streptomyces* sp. S29.** *Streptomyces* sp. S29 was able
186 to produce twelve new acyl DFO-Bs similar to those previously described.[38,39] Of these
187 12, five were short acyl chain derivatives (C_3, C_4, C_4 hydroxylated, C_5, and C_6), five were
188 monounsaturated derivatives (uC_6, uC_7, uC_{10}, uC_{11}, and uC_{12}), and two were derivatives
189 containing glutaric acid at the C-terminus, similar to those seen by Rütschlin et al.[40]
190 Pertaining to the unsaturated derivatives, placement of the alkene at the position α to the
191 carbonyl is based off previous studies also reporting DFOs containing unsaturated acyl
192 chains.[41] Additionally, the position of the hydroxy in the C_4 derivative was based on
193 previous work showing multiple amphiphilic peptide-based siderophores contain
194 hydroxylation at the β-position.[27,42]

195 We propose henceforth that the previously known 'acyl DFOs' should be renamed
196 'acyl DFO-B' due to the observation in this study of analogues that contain a *N*-acetyl-*N*-
197 hydroxycadaverine terminus, similar to desferrioxamine D. The new acyl DFO-D
198 analogues discovered here also range from short, medium and long acyl chained
199 derivatives (Table 1). It is likely the acyl DFOs are branched analogues as previous
200 studies noted that it was unlikely the chains were fully linear since *Streptomyces* spp.
201 utilise branched starter units in fatty acid synthesis.[43] This is also the case for the suite of
202 tenacibactin analogues observed in the data. These branched acyl chain siderophores
203 were originally observed in *Tenacibaculum* sp. A4K-17 [44], and are essentially truncated
204 versions of acyl DFO-Bs that lack the N-terminal *N*-hydroxycadaverine.

205 *Streptomyces coelicolor* has shown broad substrate specificity in regard to medium
206 and long acyl chain incorporation into desferrioxamine structures[19], but not short acyl
207 chained groups, where *Streptomyces* sp. S29 can facilitate production of short, medium,

208 and long acyl chained DFO-B analogues. Traxler et al. showed the ability of other
209 actinobacteria to react to the presence of *S. coelicolor*. through the production of acyl
210 DFO-B analogues.[19] Interestingly, we see this same phenomenon for the coculture of
211 *Streptomyces* sp. S29 and the fungi. Medium and long chained acyl DFO-Bs (including
212 unsaturated derivatives) were almost exclusively produced in coculture whereas short,
213 medium and long chained acyl DFO-Ds were produced under both mono- and coculture
214 conditions. The tenacibactin analogues were distributed amongst both cultures (Table 1).
215 It was hypothesized these long-chained derivatives might be a way for the uptake of these
216 analogues to bypass the DesE uptake mechanism, instead they 'hand-off' the Fe(III) via
217 membrane bound ferrioxamines.[19,45]

218 **Aryl DFO production by *Streptomyces* sp. S29.** The production of seven new
219 aryl DFOs related to legonoxamine A and B, which were also observed in this study (Table
220 1), shows the biosynthetic flexibility of *Streptomyces* sp. S29. These structures range
221 from being smaller, potential oligomers like legonoxamine C (*m/z* 351.1912, Figure S12)
222 to the larger legonoxamine H (*m/z* 665.3893, Figure S17). A few interesting legonoxamine
223 derivatives include legonoxamine F (Figure S15), putrescine-containing legonoxamine G
224 (Figure S15) and legonoxamine A glycoside (Figure S18).

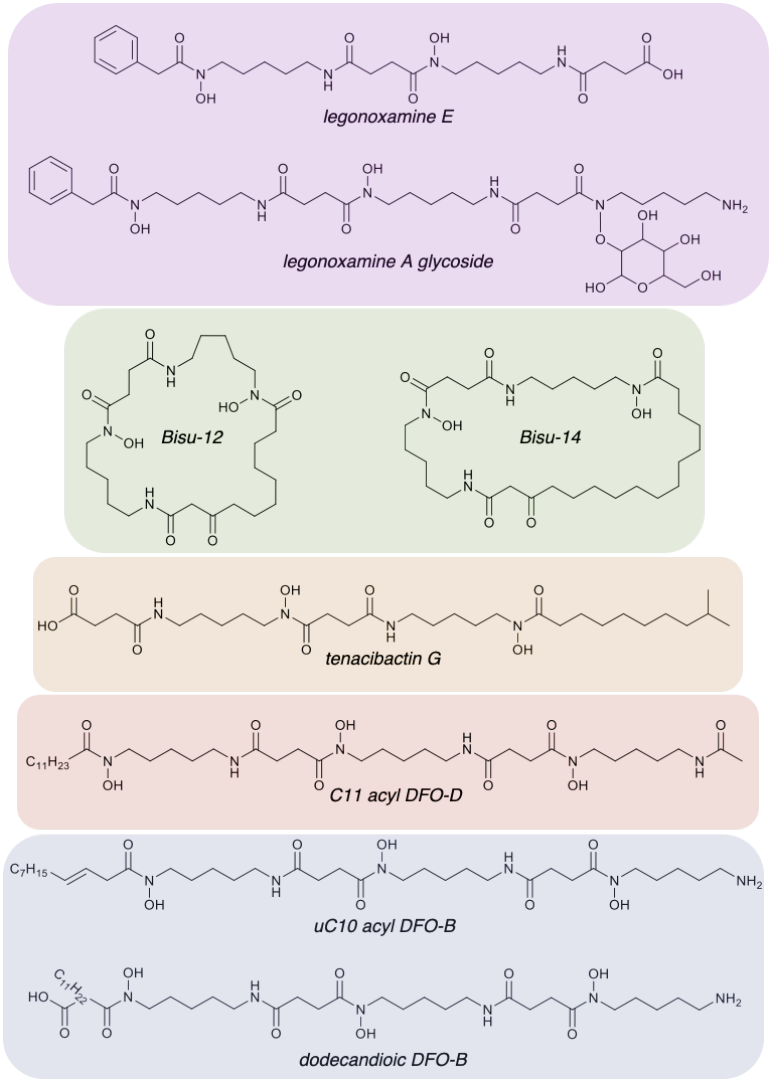

Figure 5. Representation of desferrioxamine structural diversity of *Streptomyces* sp. S29. (A-B) New legonoxamine derivatives (purple), cyclic desferrioxamines (green), tenacibactins (orange), DFO-Ds (red), and a variety of DFO-Bs (blue) were all found. Full MS/MS data and annotations can be found in supplementary for all 46 new analogues discovered.

225

226 Legonoxamine F contains one 1,6-diaminohexane instead of the typical 1,5-
227 diaminopentane. This is a well-established phenomenon in siderophore biosynthesis[28]
228 linking it to the promiscuity of the S29 *des* biosynthetic gene cluster. Legonoxamine G
229 contains a *N*-hydroxyputrescine moiety due to the initial loss of 104 Da instead of the
230 typical 118 Da associated to *N*-hydroxycadaverine. Putrebactin is the archetypal
231 putrescine containing siderophore[46], and as its biosynthetic gene cluster has been shown
232 to lack genes coding for production of putrescine, it is assumed that instead, this precursor
233 is sequestered from metabolite pools.[47] Interestingly, researchers have also found that
234 under putrescine-depleted conditions, *Shewanella putrefaciens* shifts to producing
235 desferrioxamine B when cadaverine precursors are available.[48] In desferrioxamine
236 biosynthesis, incorporation of the putrescine precursor in desferrioxamine A1 has been
237 shown before in multiple species[38,39] and now in this study with the discovery of
238 legonoxamine G.

239 Legonoxamine A glycoside was observed using the predicted molecular formula
240 ($C_{37}H_{62}N_6O_{13}$) and the loss of a sugar (-162 Da). An additional putative diglycosylated
241 DFO (*m/z* 899.4827), with a predicted molecular formula of $C_{38}H_{70}N_6O_{18}$, was observed
242 in the mass spectrum but upon selected ion monitoring (SIM), produced insufficient
243 fragment ions for structural characterisation. The production of glycosylated DFOs has
244 only been reported once before: nocardamin glucuronide, isolated from *Streptomyces* sp.
245 80H647.[40] There are only a few reports of microbial enzymes that produce glucuronides[41],
246 yet, the addition of glucose or other hexoses are more commonplace in bacterial natural
247 products.[43] We propose legonoxamine A glycoside undergoes a similar glycosylation
248 mechanism to nocardamin glucuronide, occurring on a *N*-hydroxyl.

249 **Macrocyclised desferrioxamines**. The archetypal macrocyclised DFO is
250 desferrioxamine E and has been isolated from several actinobacteria. We observe
251 desferrioxamine E in the molecular network (Figure S1) as well as several other
252 macrocyclised DFOs. In Figure 3, these are anchored by bisucaberin 01 (*m/z* 443), first
253 described by Senges et al.[44] Based on the molecular formulas, fragmentation patterns
254 and the previously established structure, we observe analogues with extensions
255 extending up to 10 CH_2's (Table 1), which differ from the bisucaberins observed in the
256 Senges et al. study which reduce in size.[19] Similar to acyl DFOs, macrocyclised
257 derivatives have also shown to have flexible biosynthesis in feeding studies, including the
258 incorporation of 1,8-diaminooctane moieties.[19] There was no observation of putrebactin,
259 or avaroferrin in the culture despite the similar biosynthesis with bisucaberins and
260 desferrioxamines.

261 **Dicarboxylic acid desferrioxamine analogues.** Two new desferrioxamines,
262 observed only in coculture extracts, with dicarboxylic acid C-termini were also elucidated.
263 Dodecanedioic DFO-B (Figure S33) has an *m/z* of 745.5086, corresponding to the
264 molecular formula of $C_{36}H_{68}N_6O_{10}$. Tridecanedioic DFO-B (Figure S34) has an *m/z* of
265 759.5221, corresponding to the molecular formula of $C_{37}H_{70}N_6O_{10}$. This is the first
266 reported instance of large dicarboxylic acids being incorporated into DFO structures yet
267 there are examples of larger dicarboxylic acids being bound to CoA, like pimelic acid,
268 therefore we cannot rule the possibility out.

269 Microbial cytochrome p450s are responsible for adding complexity to fatty acids to
270 be used as building blocks for more complex metabolites or as signalling molecules.[49]
271 Previous studies have shown the bacterial production of dicarboxylic acids might occur

272 via cytochrome p450 monoxygenase.[50] In order to determine the presence of enzymes
273 that facilitate ω-oxidation in S29, protein sequences that belong to the long-chain fatty
274 acid ω-monooxygenase enzyme class (EC 1.14.14.80) and from fatty acid ω-oxidation
275 gene ontology (GO:0010430) were obtained from the Uniprot database. BLAST results
276 of these sequences against the S29 draft genome reveals just one hit (supplementary
277 data), comprising 3 orthologs with mid-term amino acid identity (40-50%), a methyl-
278 branched lipid ω-hydroxylase (cyp124) from Mycobacterium spp. (~43% identity) (Uniprot:
279 P9WPP2, P0A517 & P9WPP3). Pfam sequence search confirms cytochrome P450
280 domain for this protein and further experimentation could confirm its ω-monooxygenase
281 activity. Searching Uniprot under these search criteria returns only a handful of bacterial
282 sequences with a couple belonging to actinobacteria, therefore, the possibilities to track
283 this activity in the S29 genome are very narrow resulting in an inconclusive result
284 regarding the presence of an ω-monooxygenase in S29.

285 **Ferrioxamines and DFO presence in pure and coculture experiments.** A
286 number of metal complexed ferrioxamines were observed in subnetwork 2 (Figure 6).
287 Fe(III) and Al^{3+} are the only metals complexed with the variety of desferrioxamines
288 present, similar to studies before.[19,45] Although the binding affinity for Fe(III) is greater
289 than Al(III)[28], it appears that this difference in affinity is not enough to prevent Al(III)
290 chelation.[46] The importance of iron has already been addressed in regard to bacteria and
291 cell maintenance but Al(III) is toxic and has no direct role in metabolism and seems to be
292 an consequence of the chemical ecology of these metabolites.

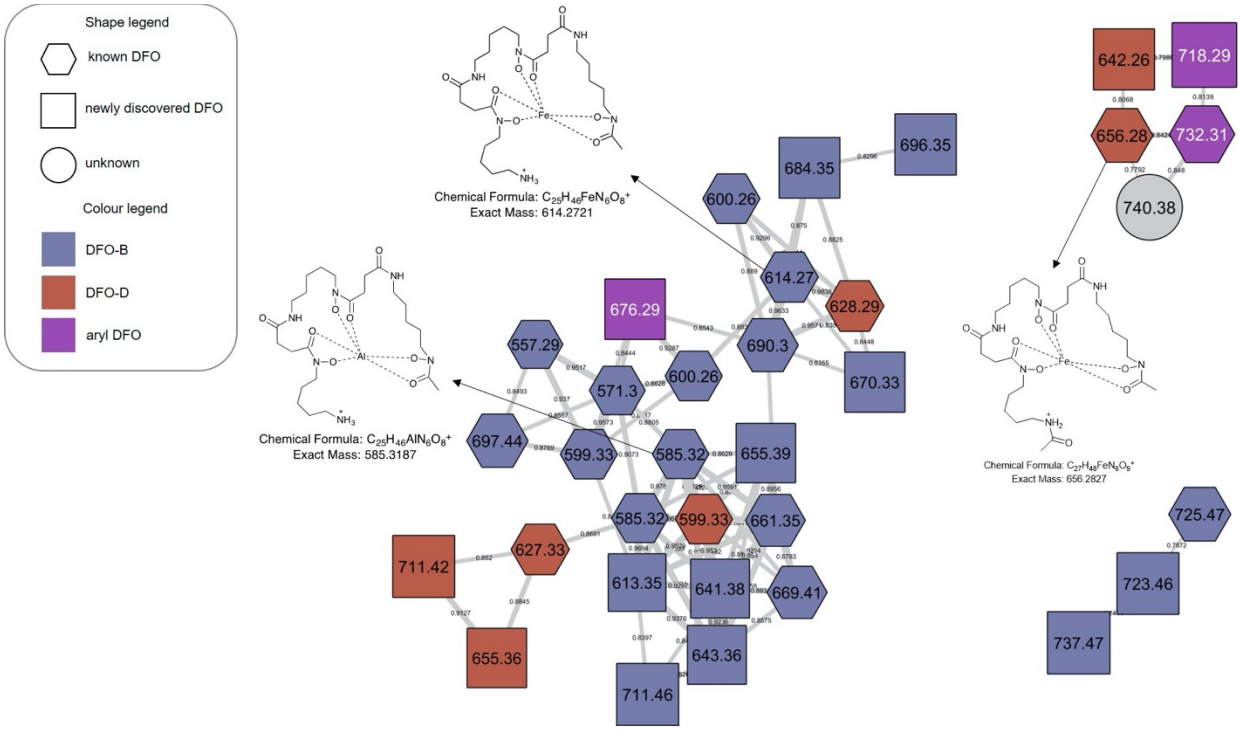

Figure 6. Metal-complexed molecular families. The GNPS library was able to identify multiple metal ion complexes (hexagonal nodes). All other features observed in the molecular network were assignable as Fe(III) or Al(III) bound ferrioxamines. Al(III) analogue of new desferrioxamine analogue –uC12 acyl FO-B. Table S1 contains accurate mass information on all complexed ions found in this figure.

The molecular network was also used to evaluate the production of the DFOs between the two cocultivations with *A. niger* and *B. cinerea* and the *Streptomyces* sp. S29 monoculture (Figure S3). The results showed that 32 of the 71 were present in the monoculture, whereas all of the remaining were found in coculture extracts only (Table 1). There was no qualitative significant difference in the siderophores produced under cocultivation with *A. niger* compared to those produced in cocultivation with *B. cinerea*, indicating the potential broad response to a fungal microbe in the environment. These results might point to DFO and siderophore production in a broader context as a common chemical response to other microbes, whether it be bacterial or fungal, in close environmental proximity to the primary organism.

304 **MS2LDA analysis.** In order to further evaluate the overall chemical space that
305 DFOs inhabit in the molecular network, MS2LDA was performed. MS2LDA is a technique
306 which identifies molecular 'fingerprints' in fragmentation patterns and assigns these into
307 motifs (13 Mass2Motifs were manually curated). By merging the two networks (GNPS
308 molecular network and MS2LDA) after motifs were annotated, it is clear that further DFO
309 chemical space is there to be discovered. Figure S4 represents the overall results of this
310 merged network where we have highlighted the previously identified features (107) and
311 edges (970) from the original molecular networking job and all of the nodes (351) and
312 edges (1991) that contain DFO motifs identified through MS2LDA. This near tripling of
313 features by inclusion of the MS2LDA workflow doesn't necessarily correlate to an
314 increase in metabolites, but upon validation of the data, there seems to be very minimal
315 features corresponding to isotopes or adducts.

316 In order to evaluate the accuracy of this analysis, a characterized DFO in this study
317 (legonoxamine E, Figure 5) and an unknown DFO observed using MS2LDA (*m/z* 650.37,
318 $[M+2H]^{2+}$) were more closely analysed (Figure S5). The unknown desferrioxamine is a
319 singleton (Figure S5B) in both the original network and the merged network, yet, MS2LDA
320 identifies it contains DFO motifs and upon closer inspection and prediction of its molecular
321 formula ($C_{59}H_{103}N_{12}O_{20}$). The potential of this putative DFO being a dimer was ruled out
322 based on fragmentation analysis lacking the monomer. Elucidation of its full structure was
323 not able to be completed with MS/MS data alone, therefore, further studies are underway
324 to characterise its structure. Nonetheless, this example displays the utility of MS2LDA to
325 evaluate the chemical potential of a bacterium and its potential use in these types of
326 studies in the future.

327 ***Streptomyces* sp. S29 siderophore biosynthetic gene clusters.** DFOs are
328 biosynthesized by nonribosomal peptide synthetase independent siderophore (NIS)
329 pathways and the presence of at least one gene encoding a homolog to IucA/IucC has
330 become recognized as a marker of NIS biosynthetic gene clusters.[47] DFO biosynthesis is
331 encoded by the highly conserved *des* biosynthetic gene cluster (*desEFABCD* genes)
332 found in many *Streptomyces* species [48]. Using FeGenie[41], the identification of iron-related
333 genes revealed 27 siderophore biosynthesis and 11 transport related genes in the
334 *Streptomyces* sp. S29 genome. These siderophore biosynthesis related genes are
335 grouped in five biosynthetic gene clusters and antiSMASH [43] predictions reveal that three
336 of the five contain at least one gene homolog to IucA/IucC and the other two correspond
337 to NRPS dependent pathways.

338 Region 7 (Figure S53) contains a siderophore BGC in *Streptomyces* sp. S29 with
339 high homology to *desA-D* genes and to the ferric-siderophore uptake and utilization genes
340 (*desE-F*). This *des* cluster follows the same structure as many *Streptomyces* spp.,
341 including the position of iron boxes upstream putative *desE* (s29_002291) and *desA*
342 (s29_002293) genes (Fig S31). DesC of the *des* BGC from *Streptomyces* sp. S29
343 (s29_2295) exhibits high identity to DesC from S. coelicolor (72%) and to LgoC from
344 *Streptomyces* sp. MA37 (69%). In *S. coelicolor* A3(2), transcription of *des* BGC is
345 repressed by the divalent metal-dependent regulatory (DmdR) protein DmdR1 and
346 derepressed by iron limitation.[44] BLASTN/P analysis revealed a putative DmdR repressor
347 in *Streptomyces* sp. S29 (s29_002782) with 89% nucleotide and 93% amino acid identity
348 to DmdR1 (AJ271797.1 / CAC28070.1). BLASTN analyses identified eight putative

349 DmdR-binding sites (iron boxes) in *Streptomyces* sp. S29 by query of putative iron boxes
350 found upstream in different ORFs in *S. coelicolor* A3(2) genome.[19]

351 Acyltransferases involved in hydroxamate biosynthesis normally exhibit narrow
352 substrate tolerance (e.g. IucB, which shows a high degree of specificity towards acetyl-
353 CoA).[19] The array of DFOs produced by *S. coelicolor* (B, E, G1 and amphiphilic) and aryl
354 DFOs (legonoxamine A-B) produced by *Streptomyces* sp. MA37, has been attributed to
355 substrate tolerant acyltransferases DesC and LgoC. [19,45] Senges et al. acknowledged in
356 their evaluation of the *Streptomyces chartreusis* secretome that in iron depleted minimal
357 medium they also observed additional desferrioxamines produced and that the overall
358 biosynthetic potential may be much broader than what has been predicted.[28] Cloning and
359 more detailed analysis of the *Streptomyces* sp. S29 *des* gene cluster is ongoing to link
360 the chemical potential shown in this study.

361 In conclusion, the chemistry observed in the *Streptomyces* sp. S29 secretome
362 shows it potential as an agent to prevent fungal infection, evidenced by its locking away
363 of Fe(III) via overproduction of desferrioxamines. New analogues were observed in both
364 monoculture and cocultivation studies with fungal phytopathogens, *A. niger* and *B.*
365 *cinerea*. *Streptomyces* sp. S29 seems to produce an arsenal of desferrioxamine
366 analogues using any available precursor materials available whether that be putrescine,
367 cadaverine, aryl, acyl, or long chained dicarboxylates. The role of bacterial communities
368 in plant and crop protection is becoming more important due to the growing world
369 population, with a strong emphasis on improving strategies at preventing phytopathogenic
370 infection. Overall, the production of 46 new and 25 previously reported siderophores

371 indicates this *Streptomyces* sp. should be studied further for its plant protective properties
372 as a biocontrol agent.

373 **EXPERIMENTAL SECTION**

374 *Strain collection*

375 *Streptomyces* sp. S29 was isolated from a soil sample collected from Lupine plant
376 (*Lupinus oreophilus*) roots originating from a polyextreme enviroment at Quebrada
377 Nacimiento, Socaire, San Pedro de Atacama, Atacama Desert (23°37'06''S;67°50'56''W
378 - 3,646 m.a.s.l). One aliquot was heated at 100 °C for 5 min and directly sprinkled onto
379 Gause #1 and Starch-Casein plates, both complemented with nystatin, cycloheximide
380 and nalidixic acid. Another aliquot was resuspended in ¼ Ringer solution, heated at 60
381 °C for 10 min and dilutions of $10^{-1/2}$ and 10^{-1} were spread onto agar plates. Plates were
382 incubated at 30 °C for ~1 week and colonies were subcultured on ISP2 plates. Based on
383 morphological characteristics of the colony and antifungal activity experiments against *B.*
384 *cinerea* and *A. niger*, 16S rRNA sequence of S29 isolate was used to identify and confirm
385 its taxonomy using EzBioCloud database (3) (data not shown).
386

387 *Phytopathogens*

388 *Aspergillus niger* and *Botrytis cinerea*, biochemically characterized field samples, were
389 provided by Laboratorio de microbiología, Facultad de Ciencias naturales, matemática y
390 medio ambiente, Universidad Tecnológica Metropolitana (UTEM), Santiago, Chile.
391 Molecular identification of these strains was carried out by sequencing of internal

392 transcribed spacer (ITS) region amplified by PCR using universal primers ITS1 and ITS4
393 (supplementary data).
394
395 *Biological screening*
396 Preliminary antifungal screening of the lupine rhizosphere *Streptomyces* collection was
397 carried out starting from spore stocks, where Streptomyces isolates were grown on ISP2
398 at 30°C for 1 week. On PDA plates, two inverted agar plugs (different isolates) from these
399 ISP2 plates, set at 2 cm from the centre, were grown at 30°C O.N. After this, the centre
400 of the PDA plates was inoculated using 10 μL of a $5x10^4$ spores/mL spore stock of a
401 phytopathogen (*Botrytis/Fusarium*) and grown at 25°C. Inhibition observations were
402 carried out at 4, 11 and 17 days from pathogen inoculation.
403 Disc diffusion assays were adapted for the microbes tested using the Clinical and
404 Laboratory Standards Institute M44 Method for Antifungal Disk Diffusion Susceptibility
405 Testing of Yeasts.[51] Extract concentrations were standardised to 200 μg/mL for all
406 bioassays conducted.
407 In order to conduct post-fermentation streaks, 50 μL of fermentation was
408 aseptically transferred onto a ISP2 agar plate. 24- and 48-hour incubation (28°C) intervals
409 were checked for fungal growth. Due to the faster growth rate of the fungi, we would
410 expect any presence of fungal spores to lead to the observation of mycelial growth, yet
411 no fungal growth was observed.

412 *Cocultivation and extraction*

413 A set of experiments were carried out on these three organisms in order to determine the
414 effect of the fungal culture being added to the *Streptomyces* sp. (a) *Streptomyces* sp. S29
415 alone: a single colony was aseptically transferred to 100 mL of iron deficient medium
416 (ISP2), shaken at room temperature at 150 RPM for 7 days, in order to induce production
417 of siderophores. (b) *Streptomyces* sp. S29 + *Aspergillus niger*: 100 mL of bacterial culture
418 was grown for 5 days, at room temperature and shaken at 150 RPM. On the second day
419 of bacterial growth, an independent axenic culture of *A. niger* (spores) was grown for 3
420 days (10 mL of PDA liquid medium, room temperature and 150 RPM shaking). On the
421 fifth day of bacterial growth, the fungal liquid culture was transferred axenically to the
422 bacterial culture and allowed to grow an addition 2 days. (c) *Streptomyces* sp. S29 +
423 *Botrytis cinerea*: the same procedure as described in experiment b was followed.
424 Additionally, each experiment contained 3 g/50 mL of sterilised glass beads to prevent
425 aggregation. Each coculture was then scaled up to 3 L total volume in an attempt to
426 produce sufficient secondary metabolites for structure elucidation.

427 Each liquid fermentation included Diaion HP-20 resin (3 g/50 mL) that was
428 sterilised with culture medium. After 7 days, the resin was vacuum filtered, subsequently
429 washed five times with milli-q water and finally macerated exhaustively in methanol (3×).
430 The methanolic extract was then dried on a rotary evaporator and subsequently
431 underwent Kupchan partitioning.[46] Finally, the *sec*-butanol fraction underwent C18 solid-
432 phase extraction (Phenomenex), with each separation yielding 5 fractions of increasing
433 methanol and these samples were subsequently prepared for LC-MS studies.

434 The 100% methanol fractions from the *Botrytis* and *Aspergillus* co-culture were
435 subjected to further separation via reversed phase-HPLC with a Waters Sunfire C18
436 semi-preparative column (5 μM, 100Å, 250 × 10 mm) wand a solvent system of A–95/5
437 MeOH/H_2O and B-MeOH. The Agilent 1200 HPLC utilized a solvent gradient of 0% B to
438 100% B at 2.0 mL/min over 50 min.

439 *Liquid chromatography – mass spectrometry*

440 All runs were analysed using an Agilent 1290 UHPLC coupled to Bruker MAXIS II Q-ToF
441 mass spectrometer. LC utilizes a Phenomenex Kinetex XB-C_{18} (2.6 mM, 100 × 2.1 mm)
442 column with a mobile phase of 5% MeCN+0.1% formic acid to 100% MeCN+0.1% formic
443 acid in 11 min. Bruker MAXIS II has a mass range of *m/z* 100-2000, capillary voltage 4.5
444 kV, nebulizer gas 5.0 bar, dry gas 12.0 l/min, and dry temperature of 220 °C. MS/MS
445 experiments were conducted under Auto MS/MS scan mode with a step collision energy
446 from 80-200%. Samples were prepared at a concentration of 0.3 mg/mL. Raw data files
447 were analysed using Bruker Daltonics 3.6.

448 *GNPS Molecular Networking and MS2LDA*

449 A molecular network was created using the online workflow (https://ccms-
450 ucsd.github.io/GNPSDocumentation/) on the GNPS website (http://gnps.ucsd.edu). The
451 data was filtered by removing all MS/MS fragment ions within +/- 17 Da of the precursor
452 m/z. MS/MS spectra were window filtered by choosing only the top 6 fragment ions in the
453 +/- 50Da window throughout the spectrum. The precursor ion mass tolerance was set to
454 0.02 Da and a MS/MS fragment ion tolerance of 0.02 Da. A network was then created
455 where edges were filtered to have a cosine score above 0.7 and more than 5 matched

456 peaks. Further, edges between two nodes were kept in the network if and only if each of
457 the nodes appeared in each other's respective top 10 most similar nodes. Finally, the
458 maximum size of a molecular family was set to 100, and the lowest scoring edges were
459 removed from molecular families until the molecular family size was below this threshold.
460 The spectra in the network were then searched against GNPS' spectral libraries. The
461 library spectra were filtered in the same manner as the input data. All matches kept
462 between network spectra and library spectra were required to have a score above 0.7
463 and at least 6 matched peaks. All features originating from the medium/instrument blanks
464 were excluded from the final molecular network.

465 For documentation on running MS2LDA, the user is referred to the original
466 publication and guidelines, which are also present at ms2lda.org.[47] All spectral images in
467 the supplementary information were created using Metabolomics Spectrum Resolver
468 (https://metabolomics-usi.ucsd.edu/).[48]

469 All siderophores dereplicated and elucidated in this study can be found in Table 1.
470 The structure elucidation of each new derivative and its corresponding MS/MS spectra
471 were generated using Metabolomics Spectrum Resolver are displayed in the
472 supplementary information (Table S2 and Figures S7-S52). All MS/MS spectra were also
473 annotated and deposited in the GNPS library, as well as the original datasets (Table S2).

474 **All data files and workflows can be found at the links below**:

475 GNPS molecular networking job:

476 https://gnps.ucsd.edu/ProteoSAFe/status.jsp?task=3c73305ef7ed48e19cb18e50b8b6b2bd

477 MS2LDA annotation experiment: http://ms2lda.org/basicviz/summary/1319/

478 MASSIVE: doi:10.25345/C5772V

479 *Streptomyces sp. S29 genome sequencing and assembly*

480 *Streptomyces* sp. S29 total DNA was extracted from liquid culture using DNeasy
481 UltraClean Microbial Kit (Qiagen). Whole genome sequencing (WGS) of the strain was
482 performed by an Illumina MiSeq (2 x 300 PE). Nanopore sequencing was performed using
483 a Rapid Sequencing Kit (SQK-RAD004) and MinIon Flow Cell (R9.4.1). The sequence
484 was assembled using Canu, polished using Racon, Illumina dataset was mapped onto
485 the contigs using BWA mem and then corrected using Pilon. The genome was annotated
486 using NCBI pgap software (6).

487

488 **ASSOCIATED CONTENT**

489 **Supplementary Information**

490 Tables of known and new desferrioxamine derivatives and their corresponding CCMS
491 Library IDs and Metabolomics Resolver Images (Table S2), disc diffusion assay results,
492 desferrioxamine containing subnetworks, new desferrioxamine analogues with annotated
493 structures and MS^2 spectra, ITS regions for fungal phytopathogens, cytochrome p450
494 enzyme sequence.

495 **Author Contributions**

496 DLS† and ED† contributed equally to this work.

497 **Conflicts of interest**

498 There are no conflicts of interest to declare.

499 **Acknowledgements**

500 SAJ would like to thank the University of Aberdeen for funding doctoral studies through
501 and Elphinstone Scholarship. DL would like to thank the Agencia Nacional de

Investigación y Desarrollo (ANID) for funding doctoral studies through 'Beca nacional de doctorado' Scholarship. ED would like to thank the Ministry of Higher Education and Scientific Research - Sudan, together with the University of Khartoum, for joint funding of master's studies. We would like to thank to Valeria Razmilic and Jean Franco Castro for their valuable advice and work in the setup of Lupine *Streptomyces* culture collection. We would also like to thank the support team at GNPS and Justin J.J. van der Hooft at MS2LDA for help with data deposition and for help at any stage of running the relevant workflows.

References

1 R. G. Expósito, I. de Bruijn, J. Postma and J. M. Raaijmakers, *Frontiers in Microbiology*, 2017, **8**, DOI:10.3389/fmicb.2017.02529.

2 O. S. Olanrewaju and O. O. Babalola, *Applied Microbiology and Biotechnology*, 2019, **103**, 1179–1188.

3 Y. Goudjal, O. Toumatia, N. Sabaou, M. Barakate, F. Mathieu and A. Zitouni, *World Journal of Microbiology and Biotechnology*, 2013, **29**, 1821–1829.

4 S. E. Jones and M. A. Elliot, *Trends in Microbiology*, 2017, **25**, 522–531.

5 V. C. Verma, S. K. Singh and S. Prakash, *Journal of Basic Microbiology*, 2011, **51**, 550–556.

6 A. Ciancio, C. M. J. Pieterse and J. Mercado-Blanco, *Frontiers in Microbiology*, 2016, 7.

7 J. M. Whipps, *Journal of Experimental Botany*, 2001, **52**, 487–511.

8 J. Shafi, H. Tian and M. Ji, *Biotechnology and Biotechnological Equipment*, 2017, **31**, 446–459.

9 D. M. Weller, *Phytopathology*, 2007, **97**, 250–256.

10 Z. R. Suárez-Moreno, D. M. Vinchira-Villarraga, D. I. Vergara-Morales, L. Castellanos, F. A. Ramos, C. Guarnaccia, G. Degrassi, V. Venturi and N. Moreno-Sarmiento, *Frontiers in Microbiology*, 2019, **10**, DOI:10.3389/fmicb.2019.00290.

11 H. Idris, M. Goodfellow, R. Sanderson, J. A. Asenjo and A. T. Bull, *Scientific Reports*, 2017, **7**, DOI:10.1038/s41598-017-08937-4.

12 ODEPA - Oficina de Estudios y Políticas Agrarias, Vinos, https://www.odepa.gob.cl/rubros/vinos-y-alcoholes, (accessed May 26, 2020).

13 M. Sandy and A. Butler, *Chemical Reviews*, 2009, **109**, 4580–4595.

14 J. Kramer, Ö. Özkaya and R. Kümmerli, *Nature Reviews Microbiology*, 2020, **18**, 152–163.

15 R. Saha, N. Saha, R. S. Donofrio and L. L. Bestervelt, *Journal of Basic Microbiology*, 2013, **53**, 303–317.

16 B. Casentini and M. Pettine, *Applied Geochemistry*, 2010, **25**, 1688–1698.

17 K. E. Jones, K. L. Batchler, C. Zalouk and A. M. Valentine, *Inorganic Chemistry*, 2017, **56**, 1264–1272.

18 U. Neubauer, G. Furrer and R. Schulin, *European Journal of Soil Science*, 2002, **53**, 45–55.
19 J. L. Ronan, N. Kadi, S. A. McMahon, J. H. Naismith, L. M. Alkhalaf and G. L. Challis, *Philosophical Transactions of the Royal Society B: Biological Sciences*, 2018, **373**, DOI:10.1098/rstb.2017.0068.
20 T. Schupp, U. Waldmeier and M. Divers, *FEMS Microbiology Letters*, 1987, **42**, 135–139.
21 F. Barona-Gómez, U. Wong, A. E. Giannakopulos, P. J. Derrick and G. L. Challis, *Journal of the American Chemical Society*, 2004, **126**, 16282–16283.
22 A. D'Onofrio, J. M. Crawford, E. J. Stewart, K. Witt, E. Gavrish, S. Epstein, J. Clardy and K. Lewis, *Chemistry and Biology*, 2010, **17**, 254–264.
23 F. Maglangit, M. H. Tong, M. Jaspars, K. Kyeremeh and H. Deng, *Tetrahedron Letters*, 2019, **60**, 75–79.
24 R. D. Firn and C. G. Jones, *Natural Product Reports*, 2003, **20**, 382–391.
25 T. Pluháček, K. Lemr, D. Ghosh, D. Milde, J. Novák and V. Havlíček, *Mass Spectrometry Reviews*, 2016, **35**, 35–47.
26 M. F. Traxler, J. D. Watrous, T. Alexandrov, P. C. Dorrestein and R. Kolter, *mBio*, 2013, **4**, DOI:10.1128/mBio.00459-13.
27 A. M. Sidebottom, A. R. Johnson, J. A. Karty, D. J. Trader and E. E. Carlson, *ACS Chemical Biology*, 2013, **8**, 2009–2016.
28 C. H. R. Senges, A. Al-Dilaimi, D. H. Marchbank, D. Wibberg, A. Winkler, B. Haltli, M. Nowrousian, J. Kalinowski, R. G. Kerr and J. E. Bandow, *Proceedings of the National Academy of Sciences of the United States of America*, 2018, **115**, 2490–2495.
29 W. J. Moree, V. v. Phelan, C. H. Wu, N. Bandeira, D. S. Cornett, B. M. Duggan and P. C. Dorrestein, *Proceedings of the National Academy of Sciences of the United States of America*, 2012, **109**, 13811–13816.
30 T. J. Telfer, M. P. Gotsbacher, C. Z. Soe and R. Codd, *ACS Chemical Biology*, 2016, **11**, 1452–1462.
31 N. Ejje, C. Z. Soe, J. Gu and R. Codd, *Metallomics*, 2013, **5**, 1519–1528.
32 M. Wang, J. J. Carver, V. v. Phelan, L. M. Sanchez, N. Garg, Y. Peng, D. D. Nguyen, J. Watrous, C. A. Kapono, T. Luzzatto-Knaan, C. Porto, A. Bouslimani, A. v. Melnik, M. J. Meehan, W. T. Liu, M. Crüsemann, P. D. Boudreau, E. Esquenazi, M. Sandoval-Calderón, R. D. Kersten, L. A. Pace, R. A. Quinn, K. R. Duncan, C. C. Hsu, D. J. Floros, R. G. Gavilan, K. Kleigrewe, T. Northen, R. J. Dutton, D. Parrot, E. E. Carlson, B. Aigle, C. F. Michelsen, L. Jelsbak, C. Sohlenkamp, P. Pevzner, A. Edlund, J. McLean, J. Piel, B. T. Murphy, L. Gerwick, C. C. Liaw, Y. L. Yang, H. U. Humpf, M. Maansson, R. A. Keyzers, A. C. Sims, A. R. Johnson, A. M. Sidebottom, B. E. Sedio, A. Klitgaard, C. B. Larson, C. A. P. Boya, D. Torres-Mendoza, D. J. Gonzalez, D. B. Silva, L. M. Marques, D. P. Demarque, E. Pociute, E. C. O'Neill, E. Briand, E. J. N. Helfrich, E. A. Granatosky, E. Glukhov, F. Ryffel, H. Houson, H. Mohimani, J. J. Kharbush, Y. Zeng, J. A. Vorholt, K. L. Kurita, P. Charusanti, K. L. McPhail, K. F. Nielsen, L. Vuong, M. Elfeki, M. F. Traxler, N. Engene, N. Koyama, O. B. Vining, R. Baric, R. R. Silva, S. J. Mascuch, S. Tomasi, S. Jenkins, V. Macherla, T. Hoffman, V. Agarwal, P. G. Williams, J. Dai, R. Neupane, J. Gurr, A. M. C. Rodríguez, A. Lamsa, C. Zhang, K. Dorrestein, B. M. Duggan, J. Almaliti, P. M. Allard, P. Phapale, L. F. Nothias, T. Alexandrov, M. Litaudon, J. L. Wolfender, J. E. Kyle, T. O. Metz, T. Peryea, D. T. Nguyen, D. VanLeer, P. Shinn, A. Jadhav, R. Müller, K. M. Waters, W. Shi, X. Liu, L. Zhang, R. Knight, P. R. Jensen, B. Palsson, K.

Pogliano, R. G. Linington, M. Gutiérrez, N. P. Lopes, W. H. Gerwick, B. S. Moore, P. C. Dorrestein and N. Bandeira, *Nature Biotechnology*, 2016, **34**, 828–837.

33 B. D. Corbin, E. H. Seeley, A. Raab, J. Feldmann, M. R. Miller, V. J. Torres, K. L. Anderson, B. M. Dattilo, P. M. Dunman, R. Gerads, R. M. Caprioli, W. Nacken, W. J. Chazin and E. P. Skaar, *Science*, 2008, **319**, 962–965.

34 M. G. Thompson, B. W. Corey, Y. Si, D. W. Craft and D. v. Zurawski, *Antimicrobial Agents and Chemotherapy*, 2012, **56**, 5419–5421.

35 P. A. G. Elmer and T. Reglinski, *Plant Pathology*, 2006, **55**, 155–177.

36 G. Perrone, A. Susca, G. Cozzi, K. Ehrlich, J. Varga, J. C. Frisvad, M. Meijer, P. Noonim, W. Mahakamchanakul and R. A. Samson, *Studies in Mycology*, 2007, **59**, 53–66.

37 J. H. Jang, K. Kanoh, K. Adachi, S. Matsuda and Y. Shizuri, *Journal of Natural Products*, 2007, **70**, 563–566.

38 G. L. Challis, *ChemBioChem*, 2005, **6**, 601–611.

39 N. Kadi and G. L. Challis, *Methods in Enzymology*, 2009, **458**, 431–457.

40 F. Barona-Gómez, S. Lautru, F. Francois-Xavier, P. Leblond, J. L. Pernodet and G. L. Challis, *Microbiology*, 2006, **152**, 3355–3366.

41 A. I. Garber, K. H. Nealson, A. Okamoto, S. M. McAllister, C. S. Chan, R. A. Barco and N. Merino, *Frontiers in Microbiology*, 2020, **11**, 37.

42 J. D. Martin, Yusai, I., V. V. Homann, M. G. Haygood, and A. Butler, *Journal of Biological Inorganic Chemistry*, **11**, 633-641.

43 K. Blin, S. Shaw, K. Steinke, R. Villebro, N. Ziemert, S. Y. Lee, M. H. Medema and T. Weber, *Nucleic acids research*, 2019, **47**, W81–W87.

44 F. J. Flores and J. F. Martín, *Biochemical Journal*, 2004, **380**, 497–503.

45 F. M. Maglangit, S. Alrashdi, J. Renault, L. Trembleau, C. Victoria, M. H. Tong, S. Wang, K. Kyeremeh and H. Deng, *Organic & Biomolecular Chemistry*, **18**, 2219-2222.

46 W. Houssen and M. Jaspars, in *Natural Products Isolation*, ed. A. Sarker, S.; Latfi, Z.; Gray, Humana Press, Second., 2006, p. 380.

47 J. J. J. van der Hooft, J. Wandy, M. P. Barrett, K. E. V. Burgess and S. Rogers, *Proceedings of the National Academy of Sciences of the United States of America*, 2016, **113**, 13738–13743.

48 M. Wang, S. Rogers, W. Bittremieux, C. Chen, P. C. Dorrestein, E. L. Schymanski, T. Schulze, S. Neumann and R. Meier, *bioRxiv*, 2020, DOI: https://doi.org/10.1101/2020.05.09.086066

49 I. N. A. van Bogaert, S. Groeneboer, K. Saerens and W. Soetaert, *FEBS Journal*, 2011, **278**, 206–221.

50 S. Honda Malca, D. Scheps, L. Kühnel, E. Venegas-Venegas, A. Seifert, B. M. Nestl and B. Hauer, *Chemical Communications*, 2012, **48**, 5115–5117.

51 *M44 : method for antifungal disk diffusion susceptibility testing of yeasts, 3rd edition.*, NIELSEN BOOKDATA, 2018.